analytical chemistry

Article

pubs.acs.org/ac

# Scanning Electrochemical Microscopy of DNA Hybridization on DNA Microarrays Enhanced by HRP-Modified $SiO_2$ Nanoparticles

Huajun Fan, Xiaolan Wang, Fang Jiao, Fan Zhang, Qingjiang Wang, Pingang He,* and Yuzhi Fang

Department of Chemistry, East China Normal University, Shanghai 200241, P. R. China

Supporting Information

**ABSTRACT:** Imaging of localized hybridization of nucleic acids immobilized on a glass DNA microarray was performed by means of generation collection (GC) mode scanning electrochemical microscopy (SECM). Amine-tethered oligodeoxynucleotide probes, spotted on the glass surface, were hybridized with an unmodified target sequence and a biotinylated indicator probe *via* sandwich hybridization. Spots where sequence-specific hybridization had occurred were modified by streptavidin-horseradish-peroxidase-(HRP)-wrapped $SiO_2$ nanoparticles through the biotin−streptavidin interaction. In the presence of $H_2O_2$, hydroquinone ($H_2Q$) was oxidized to benzoquinone (BQ) at the modified spot surface through the HRP catalytic reaction, and the generated BQ corresponding to the amount of target DNA was reduced in solution by an SECM tip. With this DNA microarray, a number of genes could be detected simultaneously and selectively enough to discriminate between complementary sequences and those containing base mismatches. The DNA targets at prepared spots could be imaged in SECM GC mode over a wide concentration range ($10^{-7}$−$10^{-12}$ M). This technique may find applications in genomic sequencing.

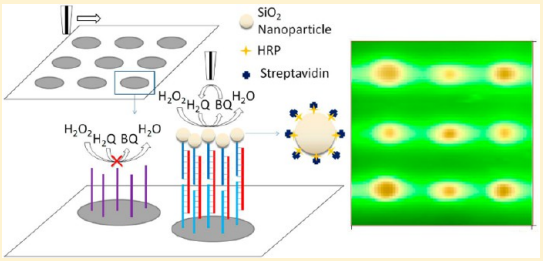


The development of parallel analytical testing platforms has led to miniaturized biosensors, biosensor arrays, and chip-based testing systems.[1−5] The biochip is a microarray device that has been developed to enable large-scale genomic, proteomic, and functional genomic analyses. Because of the benefits of low cost, high throughput, and miniaturization, this technology has great potential for clinical research, diagnostics, drug development, toxicology studies, and patient selection for clinical trials.[6−10]

DNA microarrays allow a large number of genes to be studied simultaneously. The high throughput enhances the analytical power for complicated genome analyses. They enable thousands of gene-specific sequences to be immobilized on a silicon wafer, or a nylon or glass substrate, which are then queried by copies of biological samples with radioactive or fluorescent labels.[11−15] High-density DNA arrays allow the hybridizations between the probes and the targets to be done in parallel. However, because of the small size of the hybridization array and the small amount of target present, it is a challenge to acquire signals from a DNA array. Generally, the signals must be amplified before they can be detected by imaging devices. DNA microarrays often rely on fluorescence for signal detection, which requires chemical labeling, reverse transcription, and spectroscopic instrumentation.[16,17] Recently, electrochemical detection schemes for DNA hybridization detection have been examined; they are cost-effective alternatives to fluorescence-based optical readouts since they offer high sensitivity in combination with simple instrumentation.[18−22] However, electrochemical biosensors for high throughput still present numerous challenges.

Scanning electrochemical microscopy (SECM), introduced by Bard in 1989,[23] involves current measurement through an ultramicroelectrode (UME) held above or scanned over a substrate in a solution. It is now being applied to the study of biological processes and immobilized biomolecules. The employment of SECM to characterize hybridization events on a DNA microarray is appealing because the detection sensitivity is sufficient for gene expression and it does not require special substrates. Compared with conventional electrochemical DNA sensors, application of SECM on DNA sensors realized the separation of DNA probe supporter and electrochemical signal reporter and also avoided consuming signaling species during detection. Moreover, employment of microelectrodes under steady-state conditions could eliminate problematic background currents caused by double-layer charging and possible adsorption. In addition, multiple DNA spots immobilized on insulating and conductive substrates can be studied by SECM in the presence of redox species and the spatial resolution of SECM tips matches the dimensions of DNA microarray spots. Compared with other microscopies, SECM is designed for the study of biological specimens in solution conditions close to *in vivo* and they may be interrogated repeatedly because of the nondestructive nature of the imaging process.

SECM imaging of surface-confined DNA molecules and DNA hybridization events has been reported by several groups. SECM can be used in feedback (FB) and generation collection

**Received:** April 16, 2013
**Accepted:** June 9, 2013
**Published:** June 9, 2013

**Scheme 1. Schematic of SECM Detection**

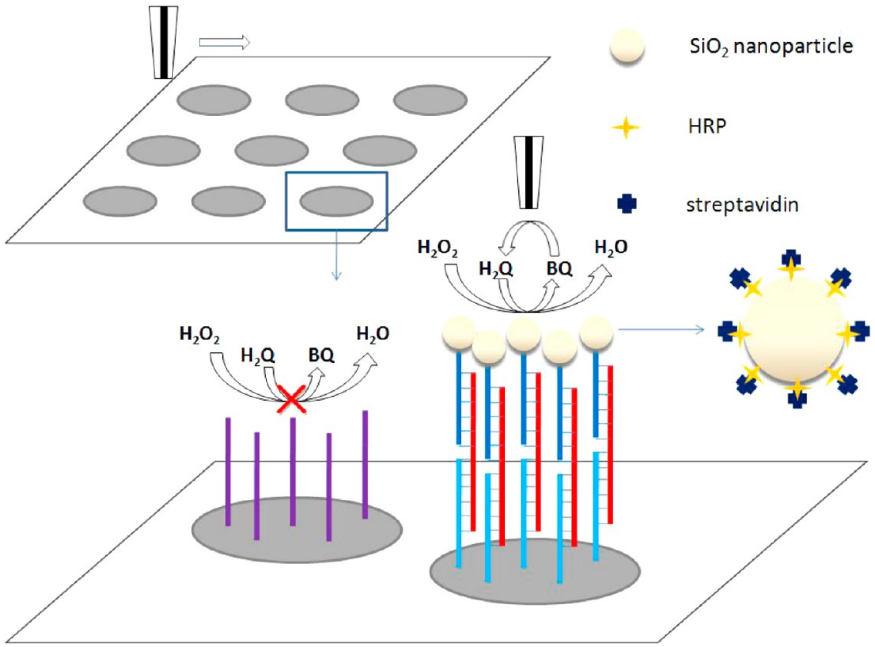


(GC) modes, and both modes have been used for imaging DNA. In the FB mode, a UME probe is used to oxidize or reduce a reversible electron mediator. Feedback occurs when the mediator diffuses to the sample and is restored to its original oxidation state through an electrochemical, chemical, or enzymatic reaction. Wain and Zhou varied the conductivities of the substrate surface using a silver staining process to allow the visualization of hybridization events on immobilized DNA spots.[24] They also reported that positive feedback currents occur on a double-stranded (ds) DNA-modified substrate *via* the redox reaction of an intercalator molecule.[25] Schuhmann and co-workers used the repulsive electrostatic forces between a negatively charged redox mediator ($[Fe(CN)_6]^{3-/4-}$) and negatively charged DNA to detect hybridization.[26,27] Kraatz et al., also using repulsive electrostatic forces, detected the presence and position of single-nucleotide mismatches in unlabeled ds-DNA films.[28] DNA hybridization could be imaged by biocatalyzed precipitation of insoluble and insulating products using horseradish peroxidase (HRP) or alkaline phosphatase.[29,30] In the GC mode, the UME detects the concentration of a particular chemical species generated at the surface of the sample, where it ideally acts only as a passive sensor for concentration mapping. The detection of DNA in the GC mode of SECM is achieved by labeled enzymes on DNA probes, such as HRP and $\beta$-galactosidase, where the redox product generated by the enzymes could be detected by the SECM tip.[31−33] Compared to the FB mode, the GC mode is more sensitive because the background signal in GC mode is very weak. In FB mode, whether in positive feedback or negative feedback, the signal must be detected against the strong background signal resulting from the hindered diffusion of the mediator from the bulk phase to the UME. Yet, the FB mode provides better lateral resolution than GC imaging because the regeneration of the mediator only occurs in close proximity to the UME.

However, multiple detection, with high sensitivity, of DNA sequences on a microarray using SECM has not been reported. Here, we describe a DNA microarray detection method with good selectivity and sensitivity by using the SG/TC (substrate generation and tip collection) mode of SECM. Compared with a fluorescence based DNA microarray device, this system offers high sensitivity in combination with simple instrumentation. The detection signal was amplified by HRP-wrapped $SiO_2$ nanoparticles (HRP-$SiO_2$). The DNA microarray was fabricated by robotic microprinting of capture DNA probes on a glass substrate. The immobilized capture probes hybridized with both the target DNA and biotinylated indicator probes, forming a "sandwich" DNA structure. Streptavidin-HRP-wrapped $SiO_2$ nanoparticles were used as the reporter element and were linked to the sandwich structure through the biotin−streptavidin interaction. Through the HRP-catalyzed reaction in the presence of $H_2O_2$, hydroquinone ($H_2Q$) was oxidized to benzoquinone (BQ) at the modified substrate surface where sequence-specific hybridization had occurred. Thus the detection was based on the reduction of BQ generated on the modified substrate by the SECM tip. The SECM detection methodology is illustrated in Scheme 1.

## EXPERIMENTAL SECTION

**Materials.** $NaH_2PO_4$, $Na_2HPO_4{\cdot}2H_2O$, NaCl, KCl, $\gamma$-glycidoxypropyltrimethoxysilane (GPMS), ethanol, acetone, cyclohexane, *n*-hexanol, tetraethoxysilane (TEOS), $NH_3{\cdot}H_2O$, ferrocenemethanol (FAM), toluene, hydroquinone ($H_2Q$), and benzoquinone (BQ) were purchased from Sigma. Triton X-100 and bovine serum albumin (BSA) were supplied by Sangon Biotech (Shanghai) Co., Ltd. Streptavidin-HRP was purchased from the Beyotime Institute of Biotechnology. All of the solutions were prepared with ultrapure water from a Millipore Milli-Q system.

DNA arrays were fabricated by robotic printing of capture DNA probes onto a glass substrate. The glass substrate was pretreated with coupling agents to immobilize the DNA; first silanization was performed, followed by hydroformylation to create modified aldehyde groups. The DNA array was 2.5 cm × 7.5 cm, and the microprinted spots were approximately 100 $\mu$m in diameter and about 200 $\mu$m apart. The DNA arrays were


dx.doi.org/10.1021/ac4011155 | *Anal. Chem.* 2013, 85, 6511−6517

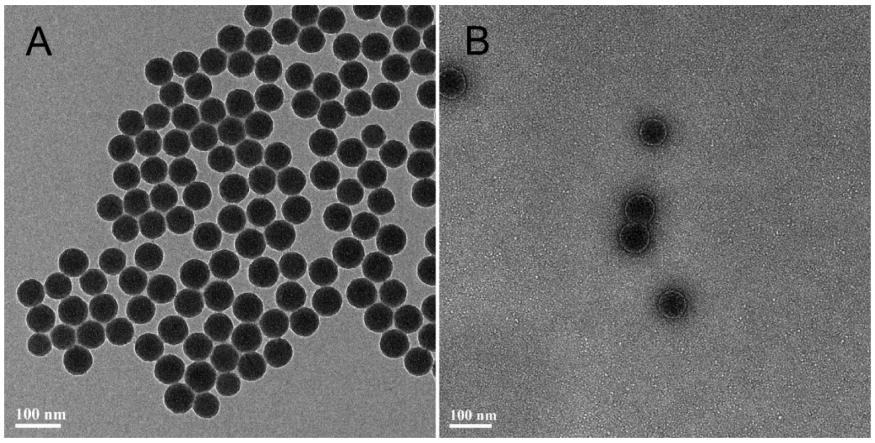


**Figure 1.** TEM images of (A) bare $SiO_2$ nanoparticles and (B) streptavidin-HRP-wrapped $SiO_2$ nanoparticles.

prepared by Shanghai Biotechnology Co., Ltd. and used as received.

Synthetic oligonucleotides (capture probes, targets, and indicator probes) were obtained from Sangon Biotech (Shanghai) Co., Ltd. The sequences of olligonucleotides were listed in the Supporting Information (Table S1). The capture probe (CP) sequences were amine-tethered oligodeoxynucleotides that could be immobilized on the aldehyde-covered glass substrate through the amine−aldehyde interaction. The concentration of CPs in the spotting procedure were 10 $\mu$M. Oligodeoxynucleotide markers for the detection of gastric cancer were selected from the National Center for Biotechnology Information as the targets. The biotinylated oligodeoxynucleotides were used as indicator probes (IP) and could link the reporter element (streptavidin-HRP-wrapped $SiO_2$ nanoparticles) through the biotin−streptavidin interaction. All oligonucleotide stock solutions were prepared in 0.1 M sodium phosphate buffer (pH 7.4) and stored at 4 °C.

**Preparation of HRP-Wrapped $SiO_2$ Nanoparticles.** The silica nanoparticles were prepared at room temperature using the reverse micelle method.[34] In brief, 7.5 mL of cyclohexane, 1.8 mL of *n*-hexanol, and 1.77 mL of Triton X-100 were continuously stirred for 5 min, and then 450 mL of deionized $H_2O$ were added to the mixture. After the mixture stirred for 30 min to form a water-in-oil microemulsion, 100 $\mu$L of TEOS and 60 $\mu$L of $NH_3{\cdot}H_2O$ (25 wt %) were slowly dripped into the continuously stirred mixture and then vigorously stirred for 24 h at room temperature. Ethanol was added to the reaction mixture to break up the microemulsion, and then the mixture was centrifuged and washed five times with ethanol and water. The particles were freeze-dried in vacuum and stored at 4 °C.

Enzyme-modified $SiO_2$ nanoparticles were formed by the amine−epoxy interaction, as follows. $SiO_2$ nanoparticles were dispersed in dry toluene by sonication for 1 h, and then 1% (V/V) GPMS was added to the solution. After shaking of the solution for 1 h at 65 °C, and then centrifugation, the epoxy groups on the surface of the nanoparticles were modified. The nanoparticles were washed sequentially with dry toluene, acetone, and ethanol and then redispersed in 1 mL of PBS (pH 7.4) and stored at 4 °C. A 450 $\mu$L aliquot of 1 mg/mL streptavidin-labeled HRP was added into the prepared epoxy-functionalized $SiO_2$ nanoparticles suspension, and the mixture was stirred at 4 °C for 10 h. Unbound streptavidin-labeled HRP was removed by washing the nanoparticles with phosphate-buffered saline solution (PBS). Finally, the nanoparticles were treated with 400 $\mu$L of 1% BSA for 24 h to block any residual epoxy groups and nonspecific binding sites on the surface. After centrifugation and washing with PBS, the HRP-$SiO_2$ nanoparticles were redispersed in 1 mL of PBS (pH 7.4) and stored at 4 °C.

**Biological Assembly for the Detection of Hybridization.** The DNA arrays were cut into small pieces and immersed in 0.1 M PBS to wet the substrate before biological assembly. Each piece was about 1 cm × 1 cm and had nine or ten DNA spots. First, the DNA array was dipped into a PBS solution with 1% BSA for 1 h to block any active sites on the substrate. After washing with 0.1 M PBS, hybridization was carried out by dropping 40 $\mu$L of 0.1 M PBS containing 0.1 $\mu$M biotinylated indicator probes and variable concentrations of targets sequences on the DNA array in a humidified chamber at 37 °C for 1 h. The volume of each target sample was 2 $\mu$L. The substrate was then washed with 0.1 M PBS to remove any nonspecifically adsorbed sequences and submerged in a PBS solution with 1% BSA for 1 h. To attach the streptavidin-HRP-modified $SiO_2$ nanoparticles, the hybridized DNA array was submerged in 400 $\mu$L of PBS solution containing 40 $\mu$L of HRP-$SiO_2$ emulsion for 1.5 h at 4 °C. Then the array was washed with PBS solution with 1% Triton X-100 to remove nonspecifically adsorbed nanoparticles and soaked in PBS at 4 °C prior to use.

**SECM Setup and Measurement.** Cyclic voltammogram (CV), approach curves, and SECM images were acquired with a model CHI 920 SECM (CH Instruments, Austin, TX, USA). The SECM instrument consists of piezo inchworms, a stage, a controller that can move the tip in three dimensions, and a bipotentiostat. A 25-$\mu$m diameter Pt UME (RG = 10) was used as an amperometric SECM tip. The reference electrode was Ag/AgCl (3 M KCl), and the counter electrode was a Pt wire. A polytetrafluoroethylene electrochemical cell was used, and the experiments were performed at room temperature. For the approach curves (tip current vs tip−substrate distance), the approach speed was 10 $\mu$m/s and the time was 50 s. Images are *x*,*y*-scans acquired at a scan rate of 100 $\mu$m/s, measuring currents in units of amperes. In this imaging experiment, according to the ratio of the increment distance (20 $\mu$m) and the increment time (0.2 s), a 1200 $\mu$m × 1200 $\mu$m area will require 12 min to scan.


dx.doi.org/10.1021/ac4011155 | *Anal. Chem.* 2013, 85, 6511−6517

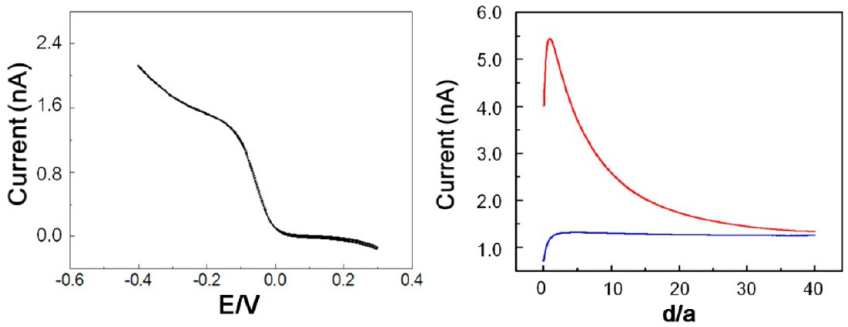


**Figure 2.** (A) Cyclic voltammogram of 1 mM BQ in 0.1 M PBS (pH 7.4) with 0.1% Triton X-100. (B) Approach curves above CP spots hybridized with (red) and without (blue) 10 nM complementary DNA in 0.1 M PBS (pH 7.4) containing 1 mM $H_2Q$, 1 mM $H_2O_2$, and 0.1% Triton X-100. The approach rate was 10 $\mu$m $s^{-1}$.

## RESULTS AND DISCUSSION

**Characteristics of the Streptavidin-HRP-Wrapped $SiO_2$ Nanoparticles.** Transmission electron microscope (TEM) images of bare $SiO_2$ nanoparticles and streptavidin-HRP-wrapped $SiO_2$ nanoparticles are shown in Figure 1. The reverse micelle synthesis of $SiO_2$ nanoparticles results in good monodispersity with an average diameter of 60 nm. Because of the large surface area of the nanoparticles, a high loading level of streptavidin-HRP is possible *via* the streptavidin−biotin interaction, thus greatly enhancing the sensitivity of the DNA probes. When compared with $SiO_2$ nanoparticle images, the streptavidin-HRP-wrapped nanoparticles exhibit a shadow and a white ring around the outer surface, indicating HRP modification.

**Evaluation of DNA Hybridization Using Approach Curves.** After the hybridization of immobilized capture DNA probes by the complementary target DNA and the biotin-labeled indicator probes, streptavidin-HRP-wrapped nanoparticles were strongly bound to the biotin labels with an affinity constant of $K_d = 10^{-15}$ $mol^{-1}$ $L^{-1}$ and suitable stability for SECM interrogation. For the HRP-catalyzed reaction, the substrate $H_2Q$ was chosen because its product BQ has excellent electrochemical properties such as a low reduction potential, negligible electrode fouling, and reversibility. Before the imaging experiment, a CV of the $H_2Q$/BQ pair and an approach curve for the DNA array substrate were obtained. Figure 2A shows the CV of 1 mM BQ in 0.1 M PBS (with 0.1% Triton X-100), with a 25-$\mu$m-diameter Pt working electrode. The CV shows the reduction of BQ to $H_2Q$, and a steady-state reduction current ($i_0$) is observed at potentials more negative than −0.3 V. Given these results, −0.4 V was chosen for SECM approach curves and imaging.

Approach curves for the DNA array were performed in 1 mM $H_2Q$ and 1 mM $H_2O_2$. With the SG/TC mode of SECM, approach curves were acquired above the CP spot hybridization with and without 10 nM target and 1 $\mu$M IP and the streptavidin-HRP-wrapped nanoparticles, as shown in Figure 2B. At the DNA spot with the target, HRP catalyzed the oxidation of $H_2Q$ to BQ with $H_2O_2$. The generated BQ diffused from the substrate to the tip, and its concentration was a function of tip−substrate distance, i.e., high near the modified substrate surface and low far from the surface. The diffusion-controlled BQ was reduced to $H_2Q$ at the Pt tip that was held at −0.4 V. Thus, the tip current ($i_T$) would increase during the approach to the substrate. As illustrated in curve 1 (red), a significant decrease in tip current occurred when the tip−substrate distance was very short. This is probably due to blocking of BQ diffusion to the tip and blocking of $H_2Q$ and $H_2O_2$ diffusion to the substrate beneath the tip, thus preventing the HRP-catalyzed reaction at the very short tip−substrate distance. The tip current reached its highest value ($i_H$) at the tip−substrate distance of 3*a* (where "a" is the tip radius, 3*a* = 15 $\mu$m), which is a balance of HRP-catalyzed reaction and diffusion inhibition. The difference between $i_H$ and the steady-state current, which we called signal current, was related to the target DNA concentration. Curve 2 (blue) was recorded above the DNA spot without the target, and where the streptavidin-HRP-wrapped nanoparticles were absent. Thus no increase in tip current was observed along the approach curve, confirming that the increase observed above the spot with target DNA was caused by HRP-catalyzed oxidation of $H_2Q$.

**SECM Imaging of DNA Microarray.** As depicted in Scheme 1, catalytic oxidation of $H_2Q$ by HRP in the presence of $H_2O_2$ at the substrate surface leads to local formation of BQ that is detected by amperometric reduction at the tip in GC mode. Ideally, the tip acts as a passive sensor to produce concentration maps of a particular chemical species near the sample surface. As the background signal is very weak, the sensitivity of the GC mode is higher than the FB mode, which represents another advantage for this study. Although the GC mode is a straightforward measurement, BQ formed close to the tip can diffuse toward the enzyme-modified substrate and be recycled to $H_2Q$, resulting in an enhancement of the total tip current. The electrochemical detection of HRP activity *via* reduction of BQ generated by HRP catalytic reaction at a movable Pt tip was previously studied by Yu et al.[33] In our work, $SiO_2$ nanoparticles were employed for enzyme immobilization to further increase the DNA detection sensitivity.

When the SG/TC mode was used for imaging DNA microarrays, an optimal working distance for imaging had to be determined that provided high sensitivity so that the SECM tip could be placed at the same position over the substrate electrode and ensure reliable results; this was accomplished by obtaining approach curves over the substrate electrode. As seen in Figure 2, during the approach, the tip current first increased and then decreased when the tip−substrate distance became shorter than 15 $\mu$m. Thus, to obtain the most sensitive signals during imaging, the SECM tip is scanned a constant 15 $\mu$m above the substrate array, while the tip current is simultaneously monitored as a function of the tip's *x*−*y* position. The dependence of the tip response on the presence of streptavidin-HRP-wrapped nanoparticle modification of the substrate reveals information about the DNA targets.


dx.doi.org/10.1021/ac4011155 | *Anal. Chem.* 2013, 85, 6511−6517

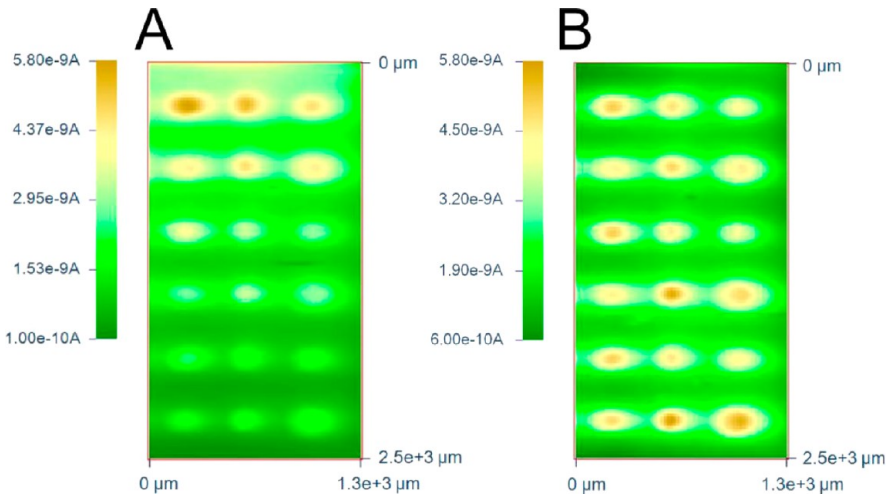


**Figure 3.** DNA array images taken (A) without 0.1% Triton X-100 and (B) with 0.1% Triton X-100.

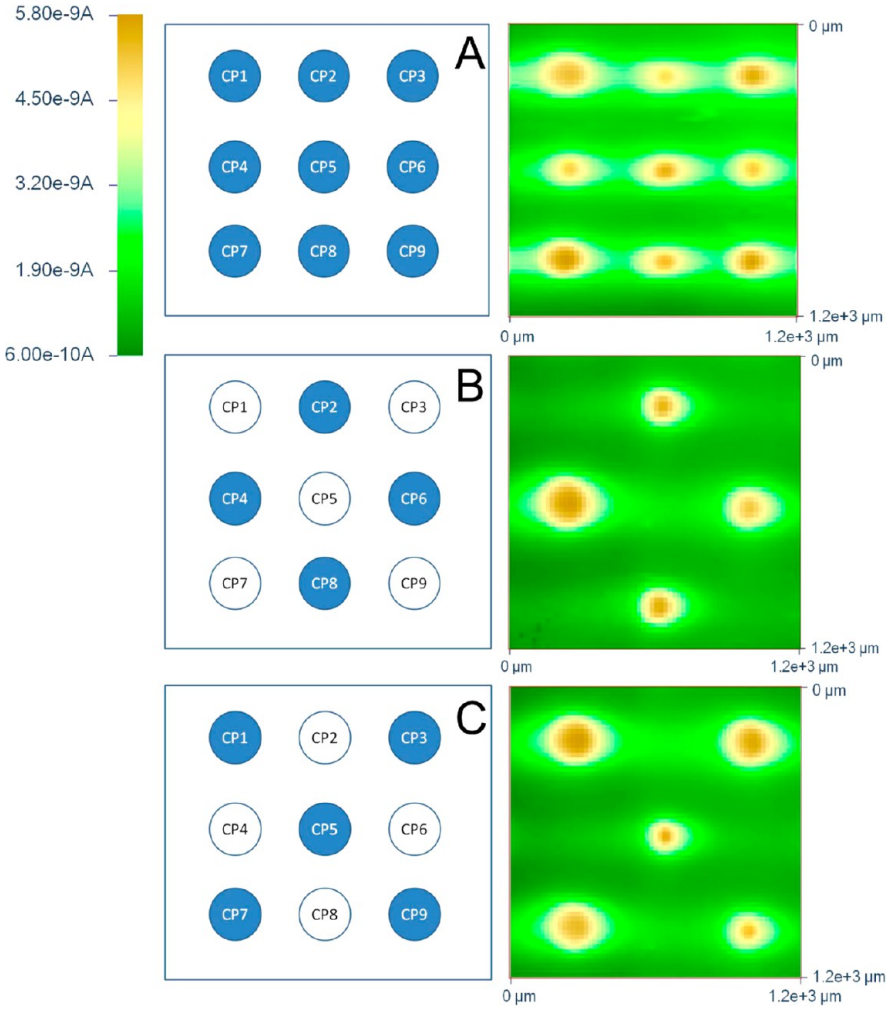


**Figure 4.** Imaging of DNA array with nine different CP spots (CP1−CP9) hybridized with targets T1−T9 (A); T2, T4, T6, T8 (B); T1, T3, T5, T7, T9 (C).

To obtain high quality SECM images of DNA microarrays, the following should be taken into account. As with any scanning probe microscopy, the surface of the substrate must be adjusted horizontally to make sure the tip is scanning at a constant height above the substrate and that the tip current background is stable (the details of substrate horizontal adjustment were illustrated in the Supporting Information). To accurately position the tip above the substrate, the 25 $\mu$m Pt tip (−0.4 V vs Ag/AgCl) was approached to the non DNA spot region. As expected, the tip current decreased during the approach, which exhibited negative feedback. The tip approach was stopped when the current had decreased to 15% of the


dx.doi.org/10.1021/ac4011155 | *Anal. Chem.* 2013, 85, 6511−6517

steady-state current, indicating that the tip was ~0.25 tip radius, or ~3 $\mu$m, away from the surface, then retreated 12 $\mu$m. In addition, passivation of the tip during scanning must be avoided. As illustrated in Figure 3A, there are 18 spots in the DNA microarray, and both the tip current background and the signal current of the DNA spots fell during scanning because of the adsorption of generated redox species on the microelectrode. To solve this problem, we added surfactant (0.1% Triton X-100) to the solution containing 1 mM $H_2Q$ and 1 mM $H_2O_2$. This keeps the tip clean during scanning by preventing the adsorption of generated redox species. An image of the DNA microarray obtained in the solution containing surfactant is shown in Figure 3B; the passivation of the tip was eliminated, and the background of the tip current was stable during scanning.

**Selectivity and Sensitivity of DNA Microarray.** As illustrated in Figure 4, we structured a small platform by spotting nine different CPs (CP1−CP9) on the glass substrate in three rows. Imaging of the array with a Pt tip held at −0.4 V versus Ag/AgCl to reduce BQ to $H_2Q$ revealed in Figure 4A nine different DNA spots, hybridized with nine targets (T1−T9) and IPs (IP1−IP9), and conjugated with streptavidin-HRP-wrapped nanoparticles. The concentration of each target was 10 nM during the hybridization. In agreement with the model, significantly heightened current levels in the central part above the DNA spot signify the high BQ concentrations generated by the HRP catalytic reaction. The tip current at the center of a DNA spot is five times higher than the tip current background. The current signal due to hybridization efficiency is not quite the same within the spots. The tip current in the region surrounding a spot is higher, probably because of the diffusion of BQ from the center to the outside of the spot, resulting in a concentration gradient. As the tip scans along the *x*-axis from left to right, the movement of the tip affects BQ diffusion, creating a horizontal band around the spots.

The DNA microarray allowed a number of genes to be studied in a single experiment. Each spot in the microarray was independent and did not affect others. When the microarray with nine different immobilized CPs was hybridized with selected targets (T2, T4, T6, T8; 10 nM), IPs (IP1−IP9) and then conjugated with streptavidin-HRP-wrapped nanoparticles, it is clear from Figure 4B that a high tip current was obtained only at spots 2, 4, 6, and 8 and that the tip current at the other spots was indistinguishable from the background. Thus the HRP catalytic reaction did not occur at the spots without targets. Similar results were obtained for a DNA microarray hybridized with selected targets T1, T3, T5, T7, T9, as illustrated in Figure 4C. Thus multiple detection of special sequence DNA was achieved in this DNA microarray.

To estimate the reproducibility and selectivity of the DNA microarray, we structured one with 10 spots in two rows. CP1 was immobilized on the five spots in row 1, while CP1′ with one base different from CP1 was immobilized on the five spots in row 2. The microarray was then hybridized with T1 (10 nM), IP1 and conjugated with streptavidin-HRP-wrapped nanoparticles. The image of the resulting array is shown in Figure 5. It is clear that the tip currents of the spots in the same row were very reproducible. Moreover, the signal currents obtained on the spots fabricated with complementary target DNA are more than five times that of the spots fabricated with one-base-mismatched target DNA. This obvious difference indicates that the hybridization with one-base-mismatched target DNA linked much fewer HRP-modified $SiO_2$ nanoparticles, leading to a reduced current at the tip. Thus, we could readily distinguish specific DNA sequences.

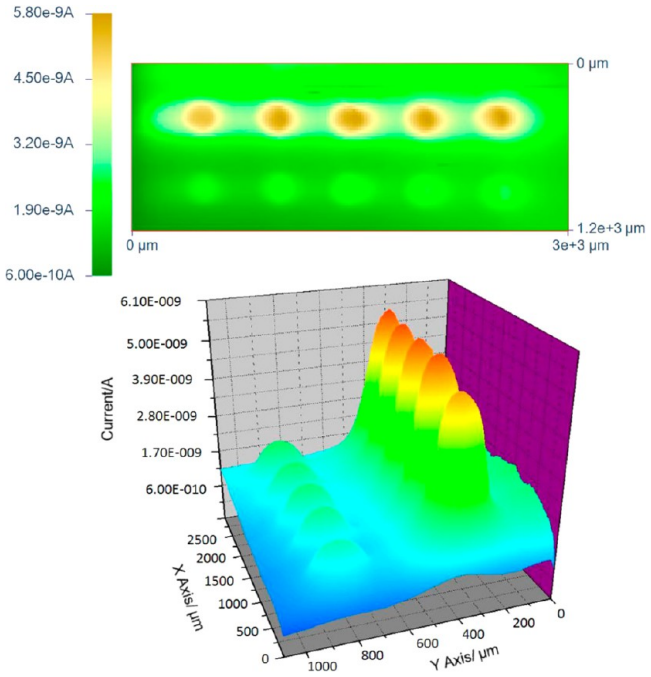


**Figure 5.** *Top*: SECM imaging of DNA spot fabricated by the hybridization with 10 nM complementary DNA (top row) and target DNA with one base mismatched sequence (bottom row). *Bottom*: 3-D plot of same.

The sensitivity of the DNA microarray was evaluated with 10 different CP spots (CP1-CP10) immobilized in two rows (Figure 6). The density of CPs on each spot was identical. The prepared DNA microarray was hybridized with different concentrations of complementary DNA targets (T1−T10) and conjugated with streptavidin-HRP-wrapped nanoparticles. The concentration of the targets varied from 100 nM to 0.1 fM ($10^{-7}$ M−$10^{-16}$ M). As clearly seen in Figure 6, better SECM

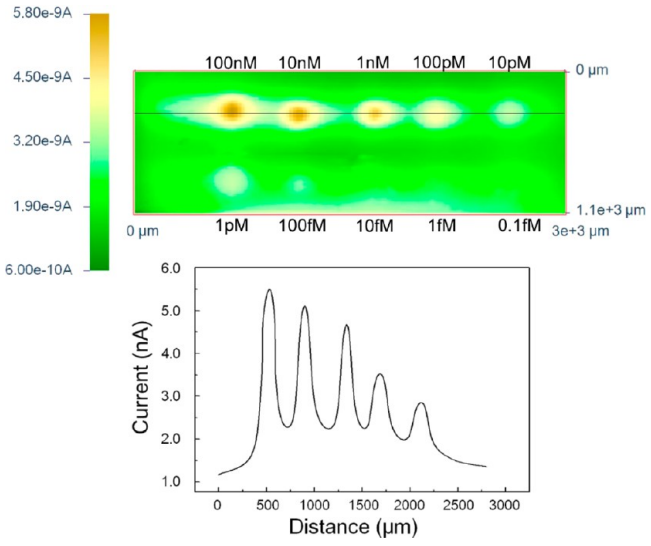


**Figure 6.** SECM imaging of DNA spots fabricated by hybridization with different concentrations (100 nM to 0.1 fM, left to right) of complementary DNA targets. *Bottom: SECM cross section line scans along the black line.*.


dx.doi.org/10.1021/ac4011155 | *Anal. Chem.* 2013, 85, 6511−6517

images of the DNA spots were acquired at higher target concentrations; the tip current at spots structured by high concentration target hybridization was high, while the signal at spots structured by low concentration target hybridization was weak. For a concentration lower than $10^{-12}$ M, almost no effect was observed and the spots were invisible in the GC mode of SECM. In this case, there were so few HRP-modified $SiO_2$ nanoparticles linked on these spots that the concentration of BQ generated on the substrate surface was too low to be detected. In contrast, the tip current signal was strong above oligonucleotide spots hybridized with 100 nM concentrated target and offered good contrast. In summary, oligonucleotide spots could be successfully visualized with the GC mode of SECM over a wide range ($10^{-7}$–$10^{-12}$ M) of target concentration.

## CONCLUSIONS

SECM imaging of localized DNA hybridization on a DNA microarray *via* the GC mode has been demonstrated. To further increase target DNA detection sensitivity, $SiO_2$ nanoparticles were employed as the carrier for enzyme immobilization to amplify the detection signal. Detection by an SECM tip was based on the reduction of BQ by an HRP-catalyzed reaction in the presence of $H_2O_2$ at the modified substrate surface where sequence-specific hybridization had occurred. Parallel analysis of multiple analytes was achieved in this study. DNA targets on prepared spots could be imaged with the GC mode in a wide range ($10^{-7}$–$10^{-12}$ M) of concentrations. This concentration sensitivity is sufficient for most applications involving gene expression and sequence analysis. Moreover, the SECM technique had good reproducibility and sufficient selectivity to distinguish complementary and one-base-mismatched sequences. Thus this system is promising for applications in genomic sequencing.

## ASSOCIATED CONTENT

### Supporting Information

Table containing sequences of capture probes, indicator probes, and targets; substrate horizontal adjustment details. This material is available free of charge via the Internet at http://pubs.acs.org.

## AUTHOR INFORMATION

### Corresponding Author

*Fax/Tel: +86-21-54340057. E-mail: pghe@chem.ecnu.edu.cn.

### Notes

The authors declare no competing financial interest.

## ACKNOWLEDGMENTS

This work was financially supported by the Natural Science Foundation of China (NSFC) (Grant Nos. 21075042 and 21275054).

## REFERENCES

(1) Whitesides, G. M. *Nature* **2006**, *442* (7101), 368–373.
(2) Corgier, B. P.; Mandon, C. A.; Le Goff, G. C.; Blum, L. J.; Marquette, C. A. *Lab Chip* **2011**, *11* (17), 3006–3010.
(3) Epstein, J. R.; Biran, I.; Walt, D. R. *Anal. Chim. Acta* **2002**, *469* (1), 3–36.
(4) Campas, M.; Katakis, I. *TrAC, Trends Anal. Chem.* **2004**, *23* (1), 49–62.
(5) Benlarbi, M.; Blum, L. J.; Marquette, C. A. *Biosens. Bioelectron.* **2012**, *38* (1), 220–225.
(6) Choucha-Snouber, L.; Aninat, C.; Grsicom, L.; Madalinski, G.; Brochot, C.; Poleni, P. E.; Razan, F.; Guillouzo, C. G.; Legallais, C.; Corlu, A.; Leclerc, E. *Biotechnol. Bioeng.* **2013**, *110* (2), 597–608.
(7) Forestier, A.; Sarrazy, F.; Caillat, S.; Vandenbrouck, Y.; Sauvaigo, S. *PLoS One* **2012**, *7* (12), doi: 10.1371/journal.pone.0051754.
(8) Zattra, E.; Zarian, H.; Peserico, A.; Saponeri, A.; Michelotto, A.; Alaibac, M. *J. Invest. Dermatol.* **2012**, *132*, S22–S22.
(9) McLaughlin, P.; Pounder, D.; Maskell, P.; Osselton, D. *Forensic Toxicol.* **2013**, *31* (1), 113–118.
(10) Hoppensteadt, D.; Litinas, E.; Khan, H.; Cunanan, J.; Thethi, I.; Iqbal, O.; Fareed, J. *Am. J. Hematol.* **2012**, *87*, S193–S193.
(11) Severin, P. M. D.; Gaub, H. E. *Small* **2012**, *8* (21), 3269–3273.
(12) Seefeld, T. H.; Halpern, A. R.; Corn, R. M. *J. Am. Chem. Soc.* **2012**, *134* (30), 12358–12361.
(13) Bailey, R. C.; Kwong, G. A.; Radu, C. G.; Witte, O. N.; Heath, J. R. *J. Am. Chem. Soc.* **2007**, *129* (7), 1959–1967.
(14) Uttamchandani, M.; Walsh, D. P.; Yao, S. Q.; Chang, Y. T. *Curr. Opin. Chem. Biol.* **2005**, *9* (1), 4–13.
(15) Schulze, H.; Barl, T.; Vase, H.; Baier, S.; Thomas, P.; Giraud, G.; Crain, J.; Bachmann, T. T. *Anal. Chem.* **2012**, *84* (11), 5080–5084.
(16) Ramsay, G. *Nat. Biotechnol.* **1998**, *16* (1), 40–44.
(17) Bentley, D. R.; Balasubramanian, S.; Swerdlow, H. P.; Smith, G. P.; Milton, J.; Brown, C. G.; Hall, K. P.; Evers, D. J.; Barnes, C. L.; Bignell, H. R.; Boutell, J. M.; et al. *Nature* **2008**, *456* (7218), 53–59.
(18) Herne, T. M.; Tarlov, M. J. *J. Am. Chem. Soc.* **1997**, *119* (38), 8916–8920.
(19) Fan, H.; Xing, R.; Xu, Y.; Wang, Q. J.; He, P. G.; Fang, Y. Z. *Electrochem. Commun.* **2010**, *12* (4), 501–504.
(20) Bakker, E. *Anal. Chem.* **2004**, *76* (12), 3285–3298.
(21) Wan, Y.; Xu, H.; Su, Y.; Zhu, X. H.; Song, S. P.; Fan, C. H. *Biosens. Bioelectron.* **2013**, *41*, 526–531.
(22) Budnikov, H. C.; Evtugyn, G. A.; Porfireva, A. V. *Talanta* **2012**, *102*, 137–155.
(23) Kwak, J.; Bard, A. J. *Anal. Chem.* **1989**, *61* (11), 1221–1227.
(24) Wang, J.; Song, F. Y.; Zhou, F. M. *Langmuir* **2002**, *18* (17), 6653–6658.
(25) Wain, A. J.; Zhou, F. M. *Langmuir* **2008**, *24* (9), 5155–5160.
(26) Turcu, F.; Schulte, A.; Hartwich, G.; Schuhmann, W. *Angew. Chem., Int. Ed.* **2004**, *43* (26), 3482–3485.
(27) Turcu, F.; Schulte, A.; Hartwich, G.; Schuhmann, W. *Biosens. Bioelectron.* **2004**, *20* (5), 925–932.
(28) Diakowski, P. M.; Kraatz, H. B. *Chem. Commun.* **2009**, *10*, 1189–1191.
(29) Fortin, E.; Mailley, P.; Lacroix, L.; Szunerits, S. *Analyst* **2006**, *131* (2), 186–193.
(30) Palchetti, I.; Laschi, S.; Marrazza, G.; Mascini, M. *Anal. Chem.* **2007**, *79* (18), 7206–7213.
(31) Kirchner, C. N.; Szunerits, S.; Wittstock, G. *Electroanalysis* **2007**, *19* (12), 1258–1267.
(32) Neugebauer, S.; Zimdars, A.; Liepold, P.; Gebala, M.; Schuhmann, W.; Hartwich, G. *ChemBioChem* **2009**, *10* (7), 1193–1199.
(33) Zhang, Z. P.; Zhou, J. Y.; Tang, A. A.; Wu, Z. Y.; Shen, G. L.; Yu, R. Q. *Biosens. Bioelectron.* **2010**, *25* (8), 1953–1957.
(34) Tang, D. P.; Su, B. L.; Tang, J.; Ren, J. J.; Chen, G. N. *Anal. Chem.* **2010**, *82* (4), 1527–1534.